

# Biogenic Amorphous Silica as Filler for Elastomers

Nikolay Dishovsky<sup>1\*</sup>, Petrunka Malinova<sup>1</sup> and Ivan Uzunov<sup>2</sup>

<sup>1</sup>University of Chemical Technology and Metallurgy – Sofia, 8 St. Kliment Ohridski Blv., 1756 Sofia, Bulgaria

<sup>2</sup>Institute of General and Inorganic Chemistry, Bulgarian Academy of Sciences, Acad. G. Bonchev Str., bl.11, 1113 Sofia, Bulgaria

Received June 15, 2017; Accepted September 17, 2017

**ABSTRACT:** Natural products from agricultural wastes are finding importance in the polymer industry due to their many advantages such as being lightweight, low cost and environmentally friendly. In the present study the potential of the two types of rice husk ash (RHA) prepared under different conditions as fillers in natural rubber-based elastomer composites was investigated. The fillers were prepared by rice husks incineration and characterized by means of X-ray powder diffraction (XRD), Fourier transform infrared spectroscopy (FTIR), scanning electron microscope (SEM), Brunauer-Emmett-Teller (BET) specific surface area, Hg-porosimetry and N<sub>2</sub>-adsorption. The evaluation involved determining the vulcanization characteristics of the compounds and their physical and mechanical characteristics, resistance to thermal aging as well as the dynamic properties of the vulcanizates containing RHA. It has been found that the ash from rice husk has good potential as filler in elastomers, especially as a substitute for synthetic commercially available silica. RHA improves the grip on ice and snow better than standard silica and may be used in formulations for shoe soles used for winter sports, extreme hiking footwear, ski boot soles, winter tire protectors, etc. Its quality depends on the conditions under which rice husk is incinerated. It is recommended to run the process at a temperature not higher than 800 °C. In particular, cases in which the vulcanizates contain biogenic silica have very interesting characteristics like improved modulus at 300% of elongation, lower residual elongation, higher mechanical loss angle tangent at 0 °C and lower at 60 °C, and are superior to those of the vulcanizates containing commercially available filler Ultrasil® 7000 GR.

**KEYWORDS:** Rice husk ash, fillers, natural rubber, mechanical characteristics, dynamic properties

## 1 INTRODUCTION

The application of various inorganic fillers significantly improves the mechanical properties of elastomers. It is well known that upon introduction of fillers the reinforcing efficiency depends, on one hand, on the complex interaction between the filler particles and the rubber macromolecules and, on the other hand, on the interaction between the filler particles themselves. The particles size and shape, their specific surface area and reactivity, the structure and uniform dispersion in the elastomeric matrix play a major role in this interaction.

In the current decade the use of materials and technologies related to renewable bio-sources at the expense of significant reduction of feedstock and petroleum-derived materials has been a major trend in the rubber industry. The increasing effort in the

development of bio-based polymeric materials in recent decades has been motivated by the concept of sustainable development of the industrial society, including by green chemistry methods. The use of bio-based fillers in polymers has been reported by a number of authors [1–3]. A comprehensive review of the latest advances in the use of bio-based composites for high-tech materials is presented in the monograph published by Smithhipong *et al.* [4]. A part of this tendency is the use of large-scale agricultural wastes as an innovative approach to utilizing environmentally friendly materials in the rubber industry. In this aspect, rice husks, a waste from rice processing, deserves particular attention. Rice is a cereal crop, a major nutrient product for a large sector of the world population. World rice production marks a steady-state trend of continuous growth—from about 20 million mt in 1960 to 600 million mt in 2004. In 2014 this quantity amounted to 741 million tons [5]. According to MAF statistical data, over the period 2010–2014 the average annual production of rice in Bulgaria was 56.5 thousand tons [6].

\*Corresponding author: dishov@uctm.edu

The initial phase of rice processing is related to the separation of rice husk waste, the amount of which is about 20 wt% of the paddy weight. That means millions of tons of waste in the form of rice husk are accumulated and managed worldwide every year. The amount of this renewable waste in Bulgaria exceeds 10 thousand tons per year.

The waste rice biomass is characterized by a high ash content, low calorific and low nutritional values making it an inappropriate feed for cattle and creating serious environmental problems [7]. Often practiced outdoors, burning of rice husk is associated with polluting the atmosphere with particulate matter, oxides of carbon, acetaldehyde, formaldehyde, etc. [8–10]. The flue gases contain a large amount of crystalline forms of silica which are hazardous to human health. At present, the problem of efficient usage of such a large scale of waste has not found a sustainable solution yet.

Systemic studies have shown that rice husk contains cellulose, hemicellulose, lignin and a significant amount of ash residue [11, 12]. A characteristic feature of rice is that its metabolism is associated with soil leaching and accumulation, mainly in the outer epidermal layer of the rice husk of silica hydrated forms. Silicon dioxide spreads to the plant in the form of monosilicic acid. As a result of water evaporation, silicic acid concentrates and participates in the formation of a silicon-cellulosic membrane, which forms a natural layer protecting the grain against pests and molds. The amount of SiO<sub>2</sub> in rice husk ranges from 18 to 23 mass percent (m%), depending on soil characteristics and agro-technical measures [13].

The high content of amorphous SiO<sub>2</sub> and carbon (~38 m%) in rice husk makes it a promising inexpensive, ecological and renewable raw source of silica and carbon. In addition, its properties, such as grain structure, chemical stability, water insolubility and high mechanical strength, are suitable for the production of value-added materials applicable in various engineering fields [14, 15].

A possible solution for the problem connected with stored renewable waste is its combustion under controlled conditions. The so-called “white ash,” the solid residue after incineration, contains more than 96 wt% of amorphous silica and reactive surface OH groups. It possesses high BET specific surface area and porous structure. The solid pyrolysis residue, obtained by pyrolysis of rice husk, is a composite material by nature. Depending on the pyrolysis temperature, it contains SiO<sub>2</sub> and carbon at different ratios.

There are versatile possibilities of using heat-treated rice husk as a filler for elastomers, e.g., white ash is used as a filler for polyethylene [16, 17], polypropylene [18–20] and polystyrene [21–23].

The aim of the present study is to evaluate the potential of the two types of rice husk ash (RHA) as fillers for natural rubber-based elastomer composites. The evaluation of that potential involves determining the vulcanization characteristics of the compounds and their physical and mechanical characteristics, resistance to thermal aging as well as the dynamic properties of the vulcanizates containing RHA.

## 2 EXPERIMENTAL

### 2.1 Used Fillers

The two types of silica produced by rice husk incineration used in this study were:

1. Silica denoted as RHA-BG was prepared under laboratory conditions at IGIC-BAS using rice husk obtained in the region of Pazardzhik, thrashing 2010. The pre-washed and dried at 120 °C rice husk was burnt in an oven at 800 °C (10° pm) in air for a 3 hour retention time. The quantity of residual carbon in the sample was determined by thermogravimetric analysis and amounted to 0.9 m%.
2. Silica designated as RHA-IND available as a commercial product was produced by N.K. Enterprises, Odisha, India. The husk temperature of combustion was about 1000 °C.
3. For comparison, standard silicon dioxide ULTRASIL® 7000 GR, manufactured by Evonik Industries, Germany, was used. This filler is used mainly for manufacturing winter tire protectors, as it provides a good grip on snowy and icy roads. The sample was labeled as 7000 GR. It is characterized by a BET surface area of 175 m<sup>2</sup>.g<sup>-1</sup>, CTAB specific surface area of 160 m<sup>2</sup>.g<sup>-1</sup> and bulk density of 270 g.l<sup>-1</sup>.

### 2.2 Analyses

The phase composition of rice husk ash was determined by X-ray analysis, performed on a Bruker D8 Advance diffractometer at Cu-K $\alpha$  radiation, in the range of 10 to 80° 2 $\theta$  degrees.

The morphology of silica was observed by scanning electron microscopy on a JEOL JSM 6390 microscope in secondary electron reflected mode (SEI), at appropriate magnification. Element surface analysis was performed on the same apparatus by energy dispersive X-ray spectroscopy (EDS).

The infrared spectra were obtained using a Nicolet Avatar 360 spectrometer in KBr pellets, at a spectral

resolution of  $2\text{ cm}^{-1}$  and 64 scan acquisitions. The spectrum was taken in the  $4000\text{--}400\text{ cm}^{-1}$  range.

The porosity and bulk density were determined by intrusive Hg-porosimetry on a Micromeritics AutoPore 9200 instrument. The differential distribution curve was determined in the 0.8 to 4995.7 psi pressure range. The porous structure was determined by low temperature ( $77.4\text{ K}$ ) nitrogen adsorption using a Quantachrome NOVA 1200 analyzer. The specific surface area was calculated by the Brunauer-Emmett-Teller equation and the pore size distribution by the Barrett-Joyner-Halenda method. The total pore volume was determined according to the Gurvich rule at a relative pressure of 0.95.

The white ash was ground in a Fritsch planetary mill in order to achieve an appropriate granulometry of the filler.

### 2.3 Preparation of the Rubber Compounds and Vulcanizates Based Thereon

The formulations of the rubber compounds designed for rubber soles of winter sports footwear and extreme hiking footwear are presented in Table 1.

The rubber compounds were prepared using an open two-roll laboratory mill (L/D  $320 \times 160$  and friction of 1.27) according to a specific recipe and blending regime. The speed of the slow roll was 25 rpm. The rubber compounds were vulcanized on an electrically heated hydraulic press with  $400 \times 400\text{ mm}$

plates at  $150\text{ }^\circ\text{C}$  and 10 MPa determined by the vulcanization isotherms taken on a MDR 2000 vulcameter (Alpha Technologies).

### 2.4 Characterization of the Vulcanizates Obtained

The compounds and the vulcanizates were characterized as follows:

- Vulcanization characteristics according to ISO 3417:2002;
- Physicomechanical parameters (modulus at 100% and 300% elongation, tensile strength, relative elongation, residual elongation) – according to ISO 37:2002;
- Shore A hardness – according to ISO 7619:2001;
- Coefficient of aging determination.

In correspondence to ISO 188-2007 the coefficient of aging was used for evaluation of heat aging resistance. It was calculated by the equation:

$$\text{Coefficient of aging} = [(X_a - X_o) / X_o] \cdot 100, \%$$

where  $X_a$  is the value of the parameter investigated (tensile strength, relative elongation, etc.) after aging;  $X_o$  is the value of the parameter investigated (tensile strength, relative elongation, etc.) before aging. The aging was carried out for 72 hours at a temperature of  $70\text{ }^\circ\text{C}$ .

**Table 1** Compositions of the rubber compounds used (in phr).

Ingredients	7000 GR	RHA-IND	RHA-BG
1. Natural rubber (STR-10)	100	100	100
2. Ultrasil® 7000 GR	60	–	–
3. RHA-IND	–	60	–
4. RHA-BG	–	–	60
5. Bis(triethoxysilylpropyl)tetrasulfide (Si 69®) – silane (coupling agent)	6	6	6
6. Process oil Werbablend® SX	25	25	25
7. Zinc oxide	3	3	3
8. Stearic acid	2	2	2
9. Polymerized trimethyl dihydroquinoline (TMQ) – anti-aging agent	1.5	1.5	1.5
10. N-(1,3-Dimethylbutyl)-N'-phenyl-p-phenylenediamine(6PPD) – anti-aging agent	0.5	0.5	0.5
11. tert-Butylbenzothiazolesulphenamide (TBBS) – accelerator	1.5	1.5	1.5
12. Diphenylguanidine – accelerator	0.5	0.5	0.5
13. Phenyl(trichloromethylsulfenyl)benzene sulfonamide (Vulkalent® E/C) – retardant	0.3	0.3	0.3
14. Sulfur (vulcanizing agent)	1.6	1.6	1.6

Dynamic properties:

- Storage modulus ( $E'$ ) and mechanical loss angle tangent ( $\tan \delta$ ) were determined at frequency of 5 Hz; 64  $\mu\text{m}$  deformation; in the  $-80$  to  $+80$   $^{\circ}\text{C}$  range at a heating rate of  $3$   $^{\circ}\text{C}\cdot\text{min}^{-1}$ . The used mode of deformation is compression. The samples were placed on a fixed flat surface and an oscillating plate applies force. The samples were 10 mm wide, 25 mm long and 2 mm thick.

The properties were determined on a Rheometric Scientific dynamic mechanical analyzer (DMA).

### 3 RESULTS AND DISCUSSION

#### 3.1 Characteristics of the Fillers Obtained by Incineration of Rice Husk

##### 3.1.1 Characteristics of RHA-BG

Figure 1a presents the X-ray diffraction analysis data of the filler. The image is typical for amorphous  $\text{SiO}_2$  [24]. The peak observed at  $2\Theta$  at about  $22^{\circ}$  is indicative of the onset of  $\text{SiO}_2$  crystalline phase formation in the sample. Under high temperature conditions, Si-O groups bound to each other yield low-temperature forms of cristobalite and tridymite [25, 26].

The FTIR data are presented in Figure 1b. Absorption peaks, typical for silica, dominate in the spectrum.

The data reveal that the silica is present in two forms:  $\alpha$ -cristobalite and tridymite. The strongest absorption band at  $1095$   $\text{cm}^{-1}$  is a singlet with weakly expressed shoulder. It is typical for the spectrum of the tridymite. The singlet bands at  $807$   $\text{cm}^{-1}$ ,  $656$   $\text{cm}^{-1}$  and  $468$   $\text{cm}^{-1}$  are characteristic for the crystal lattice of cristobalite. The broad band around  $3400$   $\text{cm}^{-1}$  is attributable to the existence of surface hydroxyl groups. The stretch band at  $1600$   $\text{cm}^{-1}$  is connected with some residues of aromatic groups C=O. The small peaks at  $2854$  and  $2920$   $\text{cm}^{-1}$  are assigned to the stretching of residual C-H methylene groups on the surface [27, 28].

The outer surface of incinerated rice husk possesses a ridged structure with a linear profile. A typical structure with prominent conical protrusions and trichomes on the outer epidermis as well as the fibrous structure of the inner epidermis are seen in Figure 2a,b.

The corrugated structure of the outer epidermis, typical for raw rice husk, was retained in the ash residue. After incineration of the lignocellulose components building the cell walls, rice husk ash retains the skeleton of polysaccharide chains wherein the dispersed amorphous  $\text{SiO}_2$  remains (Figure 2c). The thin lamellar inner epidermis appears to be undisturbed, as seen in Figure 2b. The thermal destruction of the lignocellulose matrix is associated with the intensive release of the volatile components. The volatile matter creates many pores of different sizes. They form a network of open cavities with uneven surface and irregular shape in the inner structure of RHA-BG (Figure 2d). The data from EDS analysis presented in Table 1 confirm that

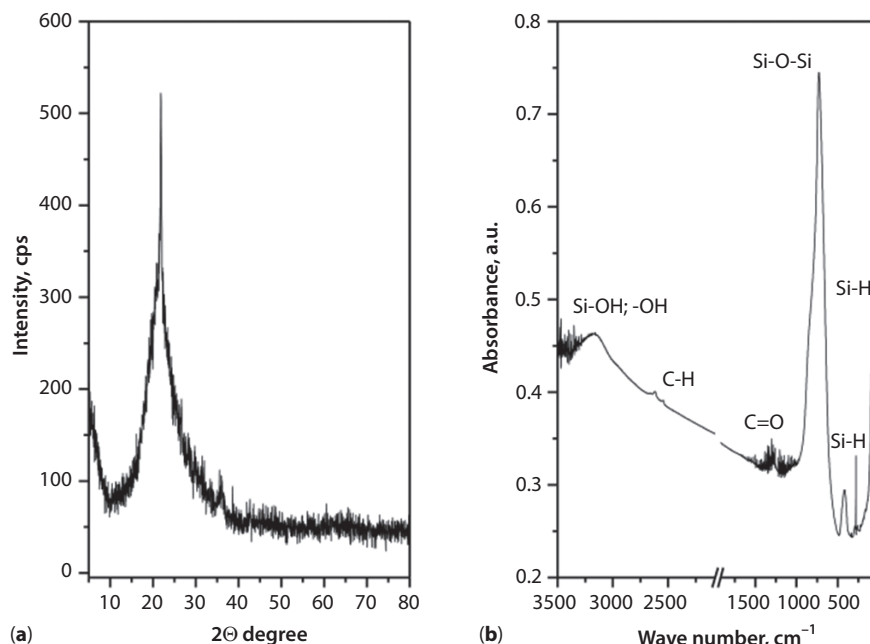
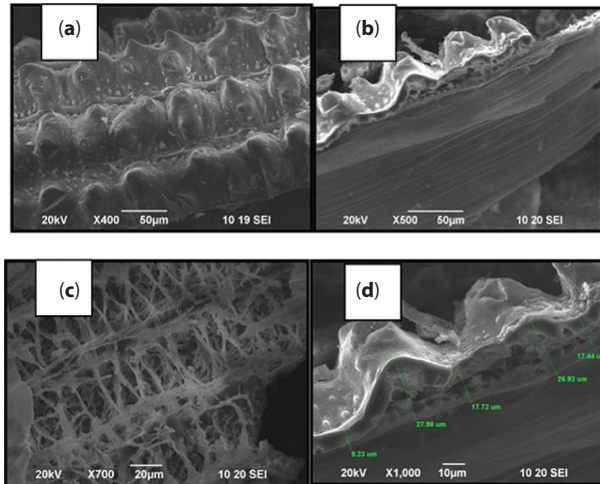


Figure 1 X-ray diffraction (a) and FTIR spectrum (b) of sample RHA-BG.



**Figure 2** SEM micrographs of RHA-BG.

the silica is concentrated predominantly in the outer surface and in a lesser amount in the inner surface of the RHA [29].

The porous structure of RHA-BG was investigated by intrusion Hg-porosimetry as well as by low-temperature adsorption of  $N_2$ . The results are presented in Figure 3 and Table 2.

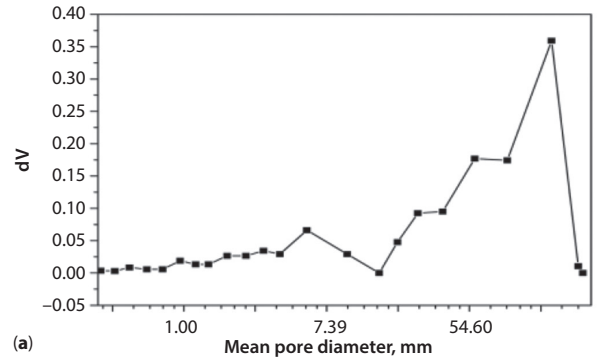
The isotherm belongs to the type V according to the IUPAC classification. It is associated with pores belonging to the 1.5–100 nm range [30]. The adsorption/desorption curve of the RHA-BG possesses a hysteresis loop which resembles the H3 type in the IUPAC classification [31]. Usually this hysteresis pattern is attributed to the crystalline agglomerates that result in the mesoporous structure formed by the interparticle space and connected with formation of secondary pores. Figure 3b reveals that the pore diameters of the sample are heterogeneously distributed in the 8–100 nm range. The calculated average pore diameter is 22.5 nm and corresponds to the mesoporous structure.

The macropores serve as transport channels facilitating a maximum contact between active sites of the filler and elastomer matrix. The analysis revealed the macropores diameter to also be heterogeneously distributed in two distinguishable ranges, 4–15  $\mu\text{m}$  and 15–250  $\mu\text{m}$  respectively (Figure 3a). The average macropores diameter was 1.47  $\mu\text{m}$ . The main structural characteristics of the RHA-BG sample are presented in Table 2.

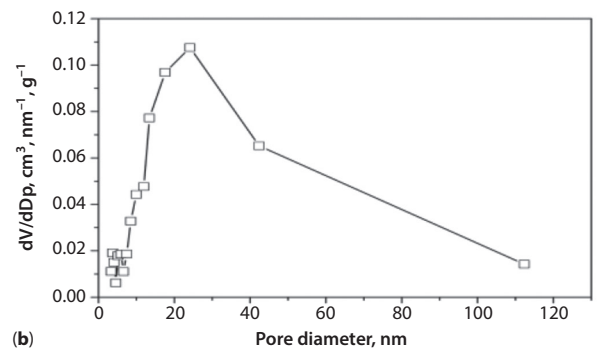
Taking into account the data obtained, the structure of RHA-BG can be defined as a multiporous one.

### 3.1.2 Characteristics of RHA-IND

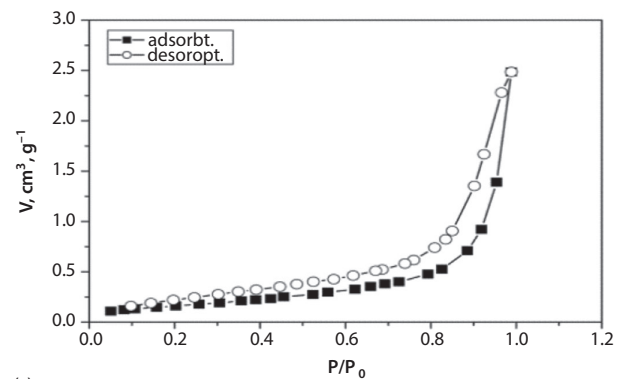
The thermogravimetric analysis data showed that the quantity of the unoxidized carbon in sample RHA-IND



(a)



(b)



(c)

**Figure 3** Pore size distribution for RHA-BG determined: (a) by Hg-porosimetry and (b) by  $N_2$  adsorption; (c) low-temperature adsorption-desorption isotherms.

**Table 2** Structural characteristics of RHA-BG.

Characteristics	Intrusion data	$N_2$ adsorption
Total pore area, $\text{m}^2 \cdot \text{g}^{-1}$	3.52	–
Average pore diameter	1.4 $\mu\text{m}$	22.4 nm
Bulk density, $\text{g} \cdot \text{cm}^{-3}$	0.49	–
Porosity, %	63.3	–
BET spec. surface area, $\text{m}^2 \cdot \text{g}^{-1}$	–	38
$V_p, \text{cm}^3 \cdot \text{g}^{-1}$	–	$7.5 \times 10^{-2}$

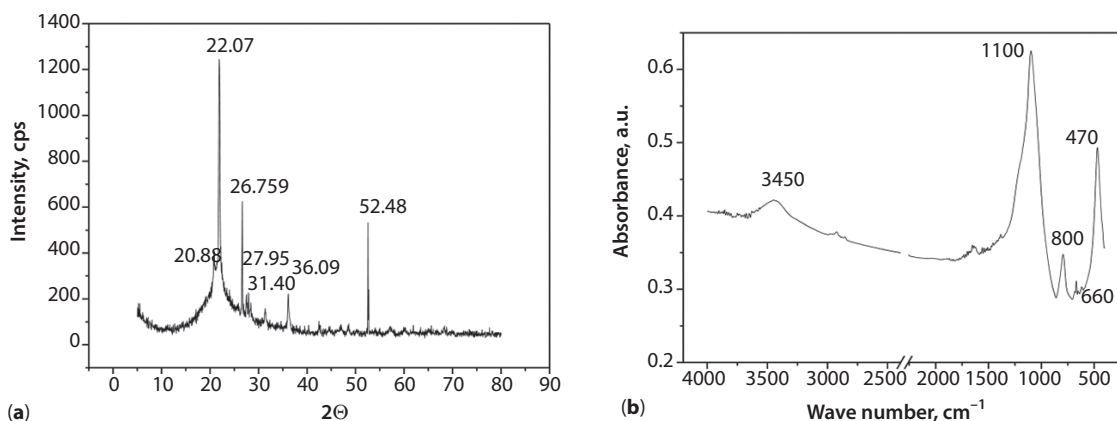


**Figure 4** XRD analysis (a) and FTIR spectra (b) of sample RHA-IND.

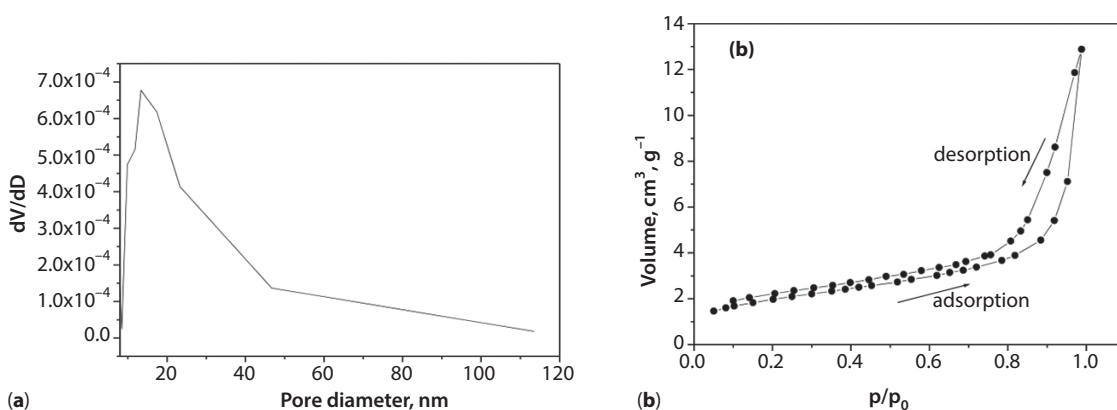


**Figure 5** Differential pore size distribution curve (a) and low temperature adsorption-desorption isotherm (b) for RHA-IND.

amounted to 3 mass %. According to XRD analysis, the filler contained mainly two phases—tridymite and cristobalite (Figure 4a).

The presence of both  $\text{SiO}_2$  forms in RHA-IND sample was also confirmed by the infrared spectroscopic data. The singlet at about  $1100\text{ cm}^{-1}$  is associated with the presence of a tridymite phase. Typical adsorption bands that refer to the presence of cristobalite are observed in the  $470\text{--}800\text{ cm}^{-1}$  range. The BET specific surface area of the material amounted to  $10\text{ m}^2\cdot\text{g}^{-1}$ .

Heterogeneous pore size distribution in the range of 10 to 50 nm was observed in the mesoporous structure of RHA-IND. The average pore diameter was 13 nm (Figure 5a). The adsorption isotherm, according to the IUPAC classification, is type V, typical for pores with dimensions up to 100 nm (Figure 5b). Crystalline agglomerates of the ash form secondary pores, which cause hysteresis in the adsorption-desorption isotherm.

The structure of RHA-IND sample is clearly seen in the SEM micrograph (Figure 6). The sample is composed of particles of irregular shapes and different sizes.

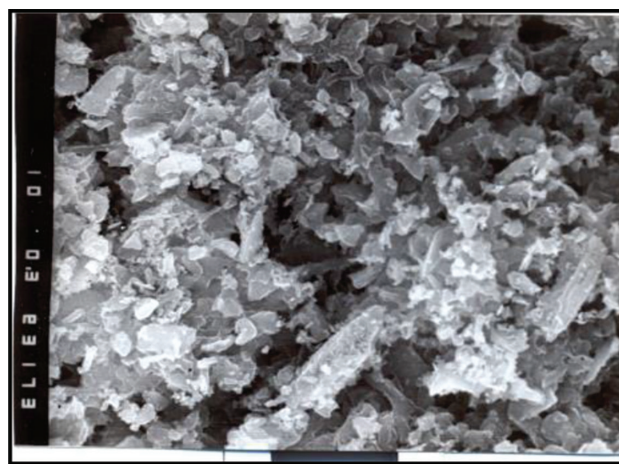


**Figure 6** SEM micrograph of RHA-IND ( $\times 10000$ ).

The obtained results revealed that the two samples have different structural and porous characteristics as well as different content of residual carbon. It follows that the physicochemical performance of the vulcanizates obtained by using the two fillers will be different.

**Table 3** Vulcanization characteristics.

Parameter	Compound code		
	GR 7000	RHA IND	RHA BG
1. ML, dN.m	1.45	0.01	0.02
2. MH, dN.m	20.80	11.36	14.54
3. $\Delta M = MH - ML$	19.35	11.35	14.52
4. $t_{s1}$ , min:sec	5:58	4:27	5:01
5. $t_{s2}$ , min:sec	7:06	4:41	5:13
6. $t_{10}$ , min:sec	7:04	4:29	5:07
7. $t_{50}$ , min:sec	9:40	5:45	6:11
8. $t_{90}$ , min:sec	15:13	12:44	12:17

Legend according to ISO 3417:2002:

ML: minimum torque correlated with the viscosity of the rubber compound;

MH: maximum torque correlated with the hardness of the rubber compound;

$\Delta M$ : related to the crosslink density of the cured compound;

$t_{s1}$ ,  $t_{s2}$ : related to the proneness of the rubber compound to scorching;

$t_{10}$ ,  $t_{50}$ : time needed for proceeding to 10% and 50% vulcanization;

$t_{90}$ : optimum vulcanization time.

### 3.2 Vulcanization Characteristics of the Compounds Containing Silica Obtained by Rice Husk Incineration

The vulcanization characteristics of the compounds containing RHA and those of the control sample are presented in Table 3.

As the results in Table 3 show, the values for certain characteristics of the compounds containing RHA-BG are closer to those of the compounds with standard (commercial) SiO<sub>2</sub> than to the ones of the compounds filled with RHA-IND. It has been established that RHA-BG filler yields compounds of a denser vulcanization network, higher hardness and resistance to scorching.

### 3.3 Physicomechanical Characteristics of the Vulcanizates Containing Silica Obtained by Rice Husk Incineration

The physicomechanical characteristics of the vulcanizates containing silica obtained by incineration of rice husk are summarized in Table 4.

The data presented in Table 4 show that the physicomechanical parameters of the vulcanizates containing RHA-BG are closer to those of the samples with standard silica than to the ones of the vulcanizates filled with RHA-IND. The samples with RHA-BG have modules at 100% and 300% elongation, tensile strength and Shore A hardness higher than those of the specimens containing RHA-IND. The latter

**Table 4** Physicomechanical characteristics of the vulcanizates.

Parameter	Compound code		
	GR 7000	RHA IND	RHA BG
1. Modulus at 100% elongation, MPa	1.9	1.2	1.5
2. Modulus at 300% elongation, MPa	7.1	4.9	7.8
3. Tensile, MPa	12.8	10.1	10.7
4. Relative elongation, %	450	450	380
5. Residual elongation, %	34	6	5
6. Shore A hardness	61	46	50

are characterized by a higher residual elongation. Regarding  $M_{300}$ , the vulcanizates with RHA-BG are 10% higher than those for the samples containing standard silica.

The reasons for the better reinforcing effect of RHA-BG are related to its structural-morphological properties predetermined by the incineration process, especially the incineration temperature, which results in:

- a lower amount of crystalline phase and higher percentage of amorphous silica;
- higher and richer surface functionality of the particles;
- retained structure, preserved from complete destruction, higher porosity guaranteeing a higher specific surface area, more points for contact between the macromolecules of the rubber and the filler particles, respectively.

The reason for the lower tensile strength and hardness of composites containing RHA in comparison to those containing standard silica may be explained as follows. It is well known [32] that the primary filler factors influencing elastomer reinforcement are: a) the primary particle size or specific surface area, which, together with loading, determines the effective contact area between the filler and the polymer matrix; b) the structure or the irregularity of the filler unit, which plays an essential role in the restrictive motion of elastomer chain under strain; c) the surface activity, which is the predominant factor with regard to filler-filler and filler-elastomer interaction. The BET surface area of the commercial silica Ultrasil 7000 GR

(used for comparison) is  $175 \text{ m}^2 \cdot \text{g}^{-1}$ , the BET surface area of RHA-IND is  $10 \text{ m}^2 \cdot \text{g}^{-1}$ , and the BET surface area of RHA-BG is  $38 \text{ m}^2 \cdot \text{g}^{-1}$ . That is why the reinforcing activity of RHA is lower than the activity of Ultrasil 7000 GR and the tensile strength and hardness are also lower.

### 3.4 Heat Aging Resistance of Vulcanizates Containing Silica Obtained by Rice Husk Incineration

The results from the studies on aging coefficients of the three samples are presented in Table 5.

The obtained data show that the vulcanizates containing standard silica Ultrasil 7000 GR are the most resistant to thermal aging, while those with RHA-BG silica are the least resistant ones. The resistance values for the samples containing RHA-IND remain close to those of the latter. The reasons for the higher resistance to thermal aging of the vulcanizates containing standard silica as well as for the different aging resistance of the vulcanizates containing the two types of rice husk silica may be due to different factors: The differences in the fillers dispersion in the elastomeric matrix, the different agglomeration in the compounding process, the peculiarities of their interaction with silane acting as a coupling agent. Another possible reason may be the bigger particle size of RHA in comparison to those of Ultrasil 7000 GR particles. It leads to bigger deformation of rubber matrix and rising internal stresses in it, which make the process of aging easier.

### 3.5 Dynamic Characteristics of the Vulcanizates Containing Silica Obtained by Incineration of Rice Husk

The dynamic mechanical thermal analysis allows determining the complex dynamic modulus  $E^*$ , storage modulus  $E'$  and loss modulus  $E''$  of a rubber material according to its reaction to strain oscillation causing sinusoidal stress. The correlation between

those parameters could be expressed by the equation  $E^* = E' + jE''$ : The ability of the composite to store energy (storage modulus measures the stored energy, representing the elastic component of the complex dynamic modulus) and its ability to lose energy (loss modulus measures the viscous component of the complex dynamic modulus) [33]. The mechanical loss angle tangent expressed by the ratio  $\text{tg} \delta = E''/E'$  is of particular importance. Its importance is on account of the definite fact that the mechanical loss angle tangent of the rubber material at  $0^\circ \text{C}$  correlates with its friction on ice and snow (the higher the tangent value, the higher the friction). In that aspect, it is worth comparing the results about the parameters of the samples containing standard silica and silica obtained by rice husk incineration. Figures 7 and 8 present the temperature dependences of the storage modulus and mechanical loss angle tangent of the studied composites in the  $-80^\circ \text{C}$  to  $100^\circ \text{C}$  range.

Figures 7 and 8 reveal the considerably different dynamic properties of the investigated vulcanizates. All three samples studied in the  $-80$  to  $-40^\circ \text{C}$  range

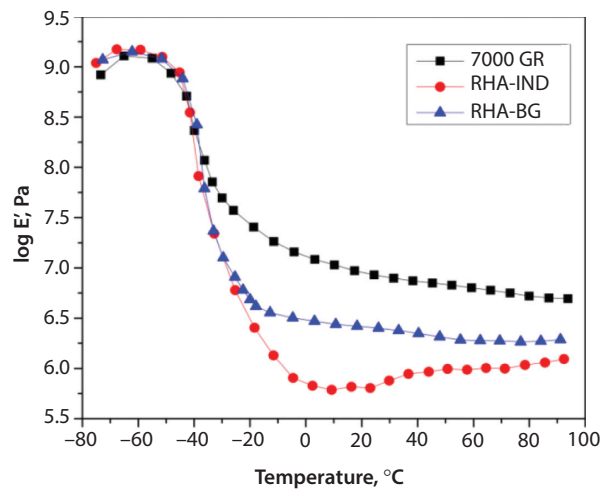
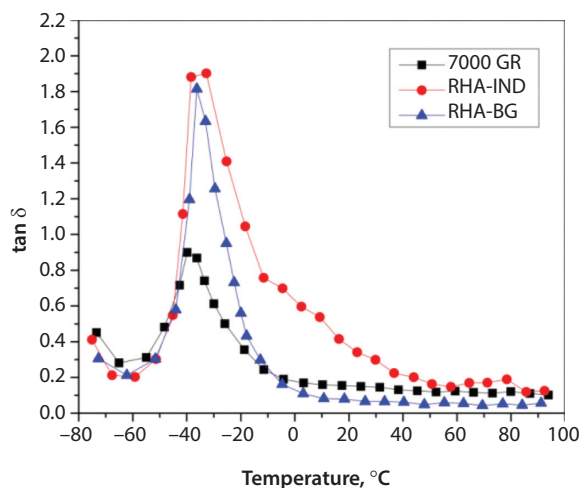


Figure 7 Temperature dependences of the storage modulus of the studied vulcanizates containing standard silica and silica obtained by rice husk incineration.

Table 5 Aging coefficients of the vulcanizates containing the three types of silica.

Parameter	Compound code		
	GR 7000	RHA IND	RHA BG
1. Aging coefficient regarding the modulus at 100% elongation, %	21	8	6
2. Aging coefficient regarding the modulus at 300% elongation, %	14	8	1
3. Aging coefficient regarding the tensile strength, %	12	-4	-16
4. Aging coefficient regarding the relative elongation, %	-2	-6	-12
3. Aging coefficient regarding residual elongation, %	-17	-12	-14
5. Changes in Shore A hardness	+2	+4	+4





**Figure 8** Temperature dependence of  $\text{tg}\delta$  of the studied vulcanizates containing standard silica and silica obtained by rice husk incineration.

are in the glass state. In this temperature range, there are no significant differences in their storage modulus. The differences, however, become serious in the  $-40$  °C to  $80$  °C range, when the vulcanizates turn into the viscoelastic state. As seen, in this interval the vulcanizates containing standard silica have the highest storage modulus values, while the samples containing RHA-IND have the lowest ones. The vulcanizates containing RHA-BG filler have intermediate values. In the  $-20$  °C to  $80$  °C range, those vulcanizates are superior to the ones filled with RHA-IND with regard to their storage modulus values and elastic properties, respectively (Figure 7). As seen from Figure 8, there is a significant difference in the glass transition temperature at which the highest tangent values are fixed. It is noteworthy that the value for RHA-BG is closer to that of standard silica than to the one for RHA-IND—the higher the mobility of the macromolecules, the lower the glass transition temperature. Marked differences are also observed in the values for mechanical loss angle tangent at  $0$  °C and  $60$  °C. It is obvious, even surprising, that the vulcanizates containing RHA-IND at  $0$  °C have values 4–5 times higher than the values for the two other samples, indicating that those vulcanizates would also have a very high friction on ice and snow, i.e., they would be suitable for winter applications (winter shoe soles, extreme hiking footwear, ski boot soles, winter tire treads, etc.), where friction on ice is very important [34, 35]. With respect to the mechanical loss angle tangent at  $60$  °C, the vulcanizates containing RHA-BG have values 2 to 2.5 times lower than those of the other samples. The following conclusion may be made about the role of RHA concerning the dynamic characteristics: It is well known that silica itself as a filler shows a very strong filler networking due to

**Table 6** Values of the mechanical loss angle tangent.

	Sample		
	7000 GR	RHA-IND	RHA-BG
Tan $\delta$ @ $0$ °C	0.20	0.60	0.15
Tan $\delta$ @ $60$ °C	0.12	0.15	0.06
Tan $\delta_{\text{max}}$	0.9 @ $-40$ °C	1.9 @ $-32$ °C	1.8 @ $-38$ °C

poor compatibility with hydrocarbon rubber, its polar character and the ability to form hydrogen bonds. The filler-filler interaction of Ultrasil 7000 GR with the surface area of  $175$  m<sup>2</sup>/g is significantly higher than that of RHA-BG and RHA-IND. On the other hand, the storage modulus  $E'$  (Figure 7) represents the stiffness of the viscoelastic material investigated and is proportional to the energy stored during a loading cycle. It is obvious that in RHA the filler-filler interaction is not very high and the stiffness of the composites containing RHA is also not very high. This is why the modulus of RHA is lower in the region  $-20$  +  $80$  °C than the modulus of Ultrasil 7000 GR. The modulus drop corresponds to an energy dissipation phenomena displayed during the relaxation process. The relaxation involves cooperative motion of long-chain sequences. The rubber modulus is known to also depend on the degree of crystallinity of the material. The crystalline regions in the natural rubber matrix (NR is a crystallizing rubber) act as physical crosslinks changing the modulus of composites, chain mobility and tangent of the mechanical loss angle. Obviously, the influence of RHA and commercially available silica on the phenomena described above is different as a result of the structure features. At the same time, a slight shift in  $T_g$  of the composites to high temperatures in the presence of RHA is observed (Figure 8). It may be due to structure irregularities of the RHA filler unit (as a result of incineration process), which play an essential role in the restrictive motion of elastomer chain under strain and shift the  $T_g$  to higher temperatures. Table 6 summarizes comparatively certain values of mechanical loss angle tangent for the investigated vulcanizates correlated with the important exploitation properties.

## 4 CONCLUSIONS

1. Certain important characteristics of elastomer compounds and vulcanizates based thereon filled with silica obtained by rice husk

incineration have been determined. The results have been compared to those from the studies on compounds and vulcanizates containing standard silica.

2. It has been found that the ash from rice husk has the potential for application as filler, especially as a substitute for synthetic silica. The conditions under which rice husk is incinerated are of great importance for the qualities of the material obtained. It is recommended that the process not be run at a temperature higher than 800 °C.
3. In particular cases the vulcanizates containing biogenic silica as filler have improved modulus at 300% of elongation, lower residual elongation, higher mechanical loss angle tangent at 0 °C and lower at 60 °C in comparison to those of the vulcanizates containing commercially available filler. This fact confirms the potential of the described new fillers for application in the rubber processing industry.
4. The results obtained show that the natural rubber-based composites containing RHA as a filler have an excellent grip on ice and may be successfully used for production of winter shoe soles, extreme hiking footwear, ski boot soles, etc.

## REFERENCES

1. S.-H. Lee and S. Wang, Biodegradable polymers/bamboo fiber biocomposite with bio-based coupling agent. *Compos. Part A-Appl. S.* **37**, 80–91 (2006).
2. L. Zhu and R. Wool, Nanoclay reinforced bio-based elastomers: Synthesis and characterization. *Polymer* **47**, 8106–8115 (2006).
3. A. Mousa, G. Heinrich, and U. Wagenknecht, Bio-based fillers, in *Encyclopedia of Polymeric Nanomaterials*, S. Kobayashi and K. Müllen (Eds.), pp. 106–109, Springer, Berlin Heidelberg (2015).
4. W. Smithhipong, R. Chollakup, and M. Nardin (Eds.), *Bio-based Composites for High-Performance Materials: From Strategy to Industrial Application*, CRC Press, Taylor & Francis Group (2015).
5. Food and Agriculture Organization of the UN, Statistics Division (EES), <http://faostat3.fao.org/>.
6. <http://www.mzh.government.bg/MZH/bg/Documents/AgrarenDoklad.aspx>.
7. V. Sergienko, L. Zemnuhova, A. Egorov, E. Shkorina, and N. Vasilijuk, Renewable sources of chemical feedstocks: Complex processing of rice and buckwheat wastes. *Russ. Chem. J.* **3**, 116–124 (2004).
8. L. Tzong-Horng, Preparation and characterization of nano-structured silica from rice husk. *Mater. Sci. Eng. A* **364**, 313–323 (2004).
9. L. Saprikin, N. Kiseleva, and Z. Temerdashev, Composition of the thermolysis products from rice husks and its hydrolytic lignin. *Wood Chemistry* **2**, 80–82 (1989).
10. W.T. Tsai, M.K. Lee, and Y.M. Chang, Fast pyrolysis of rice husk: Products yields and composition. *Bioresource Technol.* **98**, 22–28 (2007).
11. S. Chandrasekhar, K.G. Satynarayana, P.N. Pramada, P. Raghavan, and T.N. Gupta, Processing, properties and applications of reactive silica from rice husk-an overview. *J. Mater. Sci.* **38**, 3159–3168 (2003).
12. J. James and M. Subba Rao, Characterization of silica in rice husk ash. *Am. Ceram. Soc. Bull.* **65**(8), 1177–1180 (1986).
13. J. James and M. Subba Rao, Silica from rice husk through thermal decomposition. *Thermochim. Acta* **97**, 329–336 (1986).
14. V. Yakovlev, P. Yeletsky, M. Lebedev, D. Ermakov, and V. Parmon, Preparation and investigation of nanostructured carbonaceous composites from the high-ash biomass. *Chem. Eng. J.* **134**, 246–255 (2007).
15. I. Uzunov and S. Uzunova, Rice husk: Waste or valuable raw material. Possible approaches for their utilization. *Ecolog. Eng. Environ. Protect.* **3–4**, 101–112 (2013).
16. S. Panthapulakkal, S. Law, and M. Sain, Enhancement of process ability of rice husk filled high-density polyethylene composite profiles. *J. Thermoplastic Comp. Mater.* **18**, 445–458 (2005).
17. F. Yao, Q. Wu, Y. Lei, and Y. Xu, Rice straw fiber-reinforced high-density polyethylene composite: Effect of fiber type and loading. *Ind. Crops Prod.* **28**, 63–72 (2008).
18. H.G. Premalal, H. Ismail, and A. Baharin, Comparison of the mechanical properties of rice husk powder filled polypropylene composites with talc filled polypropylene composites. *Polym. Test.* **21**, 833–839 (2002).
19. S. Siriwardena, H. Ismail, and U. Ishiaku, A comparison of the mechanical properties and water adsorption behaviour of white rice husk and silica filled polypropylene composites. *J. Reinf. Plast. Comp.* **22**, 1645–1666 (2003).
20. P. Toro, R. Quijada, O. Murillo, and M. Yazdani-Pedram, Study of the morphology and mechanical properties of polypropylene composites with silica or rice-husk. *Polym. Int.* **54**, 730–734 (2005).
21. S. Siriwardena, H. Ismail, and U. Ishiaku, A comparison of white-rice husk ash and silica as fillers of ethylene-propylene-diene terpolymer vulcanizates. *Polym. Int.* **50**, 707–713 (2001).
22. H. Ismail, H. Hong, C. Ping, and H. Abdul Khalil, Polypropylene/silica/rice husk ash hybrid composites: A study on the mechanical, water absorption and morphological properties. *J. Thermoplast. Compos.* **16**, 121–137 (2003).
23. S. Siriwardena, H. Ismail, and U. Ishiaku, Water adsorption behaviour and its effect on tensile properties of ethylene-propylene-diene-terpolymer/polypropylene/filler ternary composites: A preliminary study. *Polym.-Plast. Technol. Eng.* **41**(3), 419–433 (2002).
24. M. Patel, A. Karera, and P. Prasanna, Effect of thermal and chemical treatments on carbon and silica contents in rice husk. *J. Mater. Sci.* **22**, 2457–2464 (1987).
25. F. Lanning, Silicon in rice. *Agric. Food Chem.* **11**, 435–437 (1963).

26. S. Hanna, L. Farag, and N. Mansour, Pyrolysis and combustion of treated and untreated rice hulls. *Thermochim. Acta* **81**, 77–86 (1984).
27. V. Srivastava, I. Mall, and I. Mishra, Characterization of mesoporous rice husk ash (RHA) and adsorption kinetics of metal ions from aqueous solution onto RHA. *J. Hazardous Mater. B* **134**, 257–267 (2006).
28. A. Daifullah, B. Girgis, and H. Gad, Utilization of agro-residues (rice husk) in small waste water treatment plants. *Mater. Lett.* **57**, 1723–1731 (2003).
29. B. Park, S. Wi, K. Lee, A. Singh, T-H. Yoon, and Y. Kim, Characterization of anatomical features and silica distribution in rice husk using microscopic and micro-analytical techniques. *Biomass Bioenerg.* **25**, 319–327 (2003).
30. N. Leddy, Surface area and porosity. in *CMA Analytical Workshop, Adsorption* p. 9 (2012). [http://cma.tcd.ie/misc/Surface\\_area\\_and\\_porosity.pdf](http://cma.tcd.ie/misc/Surface_area_and_porosity.pdf).
31. K. Sing and R. Williams, Physisorption hysteresis loops and the characterization of nanoporous materials. *Adsorpt. Sci. Technol.* **22**, 773–782 (2004).
32. J. Frohlich, W. Niedermeier, and H.-D. Lugisland, The effect of filler-filler and filler-elastomer interaction on the rubber reinforcement. *Compos. Part A-Appl. S.* **36**, 449–460 (2005).
33. S.R.O. Matador Rubber, *Test Methods of Rubber Materials and Products*, VERT, p.111–113 (2007).
34. M. Moncallero, S. Signetti, B. Mazzanti, P. Bruzzi, N. Pugno, and M.Colonna, Effect of material elastic properties and surface roughness on grip performance of ski boot soles under wet and icy conditions. *Int. J. Ind. Ergonomics* **61**, 62–70 (2017).
35. C. Gao, J. Abeysekera, M. Hirvonen, and C. Aschan, The effect of footwear sole abrasion on the coefficient of friction on melting and hard ice. *Int. J. Ind. Ergonomics* **31**, 323–340 (2003).